Applied Physics Letters

3D field confinement in the near-field interaction between graphene and Si/SiGe axially heterostructured NWs

Cite as: Appl. Phys. Lett. **118**, 211104 (2021); https://doi.org/10.1063/5.0050049
Submitted: 11 March 2021 • Accepted: 07 May 2021 • Published Online: 25 May 2021

Jose Luis Pura, Osman Balci, Thierry Baron, et al.

Applied Physics Letters ARTICLE scitation.org/journal/apl

3D field confinement in the near-field interaction between graphene and Si/SiGe axially heterostructured NWs

Cite as: Appl. Phys. Lett. **118**, 211104 (2021); doi: 10.1063/5.0050049
Submitted: 11 March 2021 · Accepted: 7 May 2021 ·
Published Online: 25 May 2021

Jose Luis Pura,[1,a)] Osman Balci,[2] Thierry Baron,[3] and Juan Jiménez[1]

AFFILIATIONS

[1]GdS Optronlab, Dpt. Física de la Materia Condensada, Ed. LUCIA Universidad de Valladolid, Paseo de Belén 19, 47011 Valladolid, Spain
[2]Cambridge Graphene Centre, Cambridge University, Cambridge CB3 0FA, United Kingdom
[3]University Grenoble Alpes, LTM, F-38000 Grenoble, France and CNRS, LTM, F-38000 Grenoble, France

[a)]**Author to whom correspondence should be addressed:** jlpura@fmc.uva.es

ABSTRACT

Interest in the integration of graphene and semiconductor nanowires (NWs) increased dramatically during the last two decades along with the overwhelming development of graphene technology. The possibility of combining the countless properties of graphene with the singular optical behavior of semiconductor NWs leads the way to the design of unique photonic nanodevices. In this work, the optical response of Si/SiGe axially heterostructured NWs deposited over a graphene monolayer is investigated. The results demonstrate the enhancement of the graphene Raman signal under the influence of the NW. Moreover, the presence of an axial heterojunction in the NW is shown to locally hinder this enhancement through the full confinement of the incident electromagnetic field inside the NW body around the heterojunction. This complex interaction could be the basis for near-field probes for molecules or 2D materials, and optoelectronic devices including graphene/NW interfaces.

The singular interaction of semiconductor nanowires (NWs) with electromagnetic (EM) fields can open the door for a great number of applications. NWs have been shown to present strong optical resonances connected to their characteristic dimensions, i.e., diameter and length.[1–3] Additionally, one can tune their optical properties by varying other NW properties like composition.[4] Beyond their intrinsic properties, further experimental implementations of NW-based configurations allow for extending their tunability, including additional parameters that can be modified to control the optical response, e.g., varying the pitch and disposition in NW arrays.[5,6] As a consequence of their unique optical properties, semiconductor NWs can be found in all sorts of new generation optoelectronic nanodevices,[7] including LEDs,[8,9] nanolasers,[10,11] and high-efficiency solar cells.[12–15] All these interesting properties and their corresponding applications can be tailored by controlling NW growth in order to design the required NW configuration. Furthermore, both axial and radial heterostructures can be grown in NWs without the lattice matching restrictions found in thin films.[16]

The ability of NWs to locally enhance the electromagnetic field might allow the NWs to be used as nanometric probes when deposited on different media, e.g., measuring the local thermal conductivity of thin films by the optical response of NWs deposited on them.[17] One can interface NWs with other molecules or living cells and study its optical properties,[18] or enhance the optical response of 2D layered materials by depositing NWs on them.[19]

Interest in the integration of graphene with NWs has grown following the overwhelming development of graphene technology. There have been great signs of progress on the development of hybrid graphene/NW structures for nanotechnology applications over the last decade. Interesting results can be found about the use of metallic NWs together with graphene for the elaboration of transparent conducting electrodes (TCE). Exceptional optical and electrical properties have been obtained in conjunction with high mechanical flexibility by using Cu or Ag NWs arranged with graphene in different configurations.[20,21] Graphene can also be used on ZnO NWs for UV photodetectors,[22] which provides an improved performance with respect to conventional photodetectors. Another promising field for the application of graphene/NW structures is NW-based solar cells. The transparency of graphene together with its electric conductivity allows its use for TCEs

in NW solar cells. Moreover, the electronic properties of the graphene/semiconductor junctions provide further flexibility to device design, especially the diode-like graphene/silicon Schottky junction.[23] These promising properties have led to the investigation of graphene/Si NWs solar cells,[24,25] looking for enhanced performance.

Here, we present a study of the electromagnetic coupling between Si/SiGe axially heterostructured NWs and graphene using micro-Raman spectroscopy. Graphene provides us with the possibility of having a one-atom layer of material near the NW, allowing to measure the local EM field exceptionally close to the NW surface, as well as studying the optical interaction between both nanoscale systems.

Single-layer graphene (SLG) is synthesized by chemical vapor deposition (CVD) method on a 25-μm-thick Cu foil. The resulting SLG is polycrystalline resembling the Cu foil surface. After loading the Cu foil in a CVD chamber, the system is heated to 1000 °C in 30 min under 40 sccm H_2 flow and annealed for 30 min. For the growth, 5 sccm CH_4 is introduced additionally, and the growth is terminated by stopping all gas flow after 30 min. To transfer SLG, PMMA A4 950 is spin-coated at 4000 rpm on SLG/Cu. The Cu foil is chemically etched in 44 mM ammonium persulphate aqueous solution for 5 h. Subsequently, the SLG/PMMA is kept in de-ionized water for 4 h for cleaning. The SLG/PMMA stack is transferred on the Al-coated Si/SiO_2 substrate and left for drying for 12 h. Finally, the PMMA on SLG is removed by acetone and a following isopropyl alcohol treatment. The Al thickness is ~500 nm, enough to block any Raman signal coming from the Si substrate.

Axially heterostructured $Si_{1-x}Ge_x$/Si/$Si_{1-x}Ge_x$ ($x \approx 0.6$) NWs were deposited over the graphene layer by drop-casting a methanol/NW suspension. The SiGe/Si/SiGe axially heterostructured NWs were grown by the vapor–liquid–solid (VLS) method in a low-pressure CVD reactor using SiH_4 and GeH_4 as precursors. Further details about the process can be found in previous work.[26]

Micro-Raman spectroscopy measurements were carried out with a Labram UV-HR 800 Raman spectrometer from Horiba-Jobin Yvon. The excitation and the scattered light collection were performed by means of a confocal metallographic microscope with a high magnification objective (X100) and 0.95 numerical aperture. A frequency-doubled Nd:YAG laser (532 nm) was used as the excitation source. The laser beam diameter at the focal plane is slightly below 1 μm according to the Abbe formula ($\phi = 1.22\,\lambda$/NA). The excitation power was fixed to $510 \pm 5\,\mu$W for all measurements, and the spectrum acquisition time was 10 s.

Finite element methods (FEM) simulations were performed with the commercial software COMSOL Multiphysics. The electromagnetic waves in frequency domain (EWFD) module was used to solve the Maxwell equations for the NW/graphene/substrate system under laser light illumination. The model provides the 3D distribution of the EM field intensity, $|E|^2$, which allows us to compute the expected Raman signal of each material since the Raman signal is proportional to the effective excitation light intensity.[27,28]

The first measurements were performed on graphene/SiO_2 substrate, revealing a typical graphene Raman spectrum showing its characteristic Raman bands at 1580 cm^{-1} (G band) and 2700 cm^{-1} (2D band),[29] Fig. 1(a). The intensity ratios I(2D)/I(G) = 5.2 and I(D)/I(G) = 0.4 are in good agreement with the excitation wavelength (532 nm), the absence of doping, and the polycrystallinity of SLG.[30,31] The FWHM of the 2D is ~26 cm^{-1} and remains stable throughout all the experimental measurements. When these measurements are repeated on graphene/Al-coated SiO_2 substrate, the Raman signal of graphene is dramatically quenched, (Fig. 1(a) (inset)). Figure 1(b) shows the graphene Raman signal profile when the excitation laser beam is scanned from a region over the bare SiO_2/Si substrate to an Al-coated region. This profile shows the progressive fading of the graphene Raman signal (represented by the intensity of the more intense

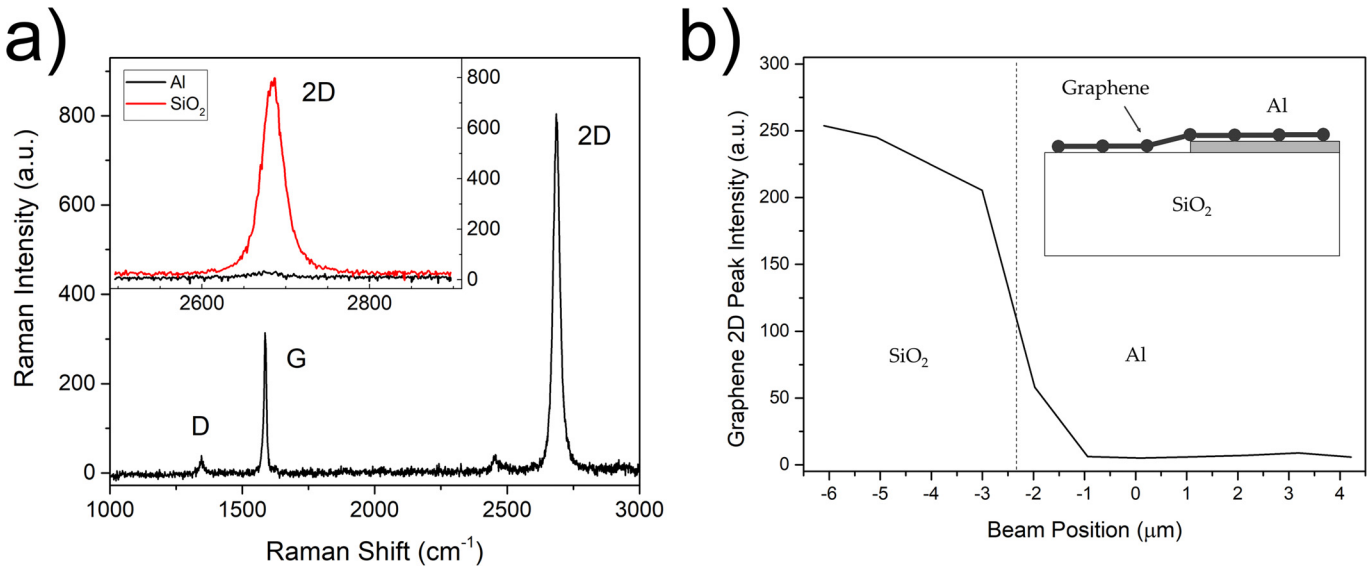

FIG. 1. (a) Typical Raman spectrum of graphene; the inset shows a comparison of the Raman signal of graphene over the bare SiO_2 substrate and the Al-coated substrate. (b) Integrated Raman intensity (2D Raman band) of the graphene layer over the transition from the SiO_2 substrate to Al. The Raman signal is quenched on Al because of its metallic nature.

2D Raman band) as the laser beam crosses from the SiO_2/Si substrate to the Al-coated substrate. This can be easily explained because Al is a metal; therefore, the electric field of an incident light wave should vanish at its surface. Since graphene is a one-atom layer, the excitation electromagnetic field should be extremely low because of its close proximity to the metal. This behavior is not observed for the graphene/SiO_2 system because as SiO_2 is an insulator and transparent to visible light, the electric field does not vanish, normally exciting the Raman signal of the graphene layer.

Let us consider what happens when NWs are deposited on graphene. The experimental measurements prove that the quenched Raman signal of the graphene/Al system is retrieved in the presence of the NW. Figure 2 shows the representative results of a transverse scanning on a SiGe/Si/SiGe NW deposited on graphene/Al across one of its SiGe segments; the Raman intensities of both, the NW (Si–Ge Raman band) and graphene (2D band), are plotted. There is a clear intensity correlation between both signals: the graphene Raman signal is severely reduced when the laser beam is out of the NW and grows up when the laser beam progressively illuminates the NW, as monitored by the NW Raman signal. This figure displays the recovery of the graphene Raman signal in the presence of the NW.

This highlights the utility of semiconductor NWs for enhancing the Raman signal of materials with nanometric spatial resolution even under unfavorable experimental conditions. This also evidences the capacity semiconductor NWs for tailoring the photon absorption.

The use of the NWs as local optical probes, when illuminated with focused laser beams, provides a spatial resolution of a few tens of nanometers; however, such resolution cannot be reached in the axial direction. This limitation could be overcome by using NWs with axial heterojunctions. We have shown in previous articles that the heterojunctions play a relevant role in the distribution of the electromagnetic field when the NW is illuminated by a laser beam. The light is concentrated around the heterojunction (HJ), providing a potential spatial resolution in the axial direction of a few tens of nanometers. In order to confirm this, a 2D laser scan of the NW was performed in order to study the role of the HJs with respect to the Raman signal of graphene. As shown in previous works,[26–28,32] the axial HJs give additional light absorption resonances enhancing the Raman signal with respect to the homogeneous segments of the NW. The results of the 2D scanning are summarized in Fig. 3. The Raman signal of graphene (2D band) is increased when the excitation beam illuminates the NW, in accordance with what was observed in the transverse scan of Fig. 2. The graphene signal level is rather homogeneous throughout the NW; however, a minimum can be observed when the laser beam runs across the Si/SiGe HJ. *A priori* we expected the graphene Raman signal to be enhanced by the HJ because of the resonance absorption at the HJ,[26,32] similarly to the SiGe Raman intensity in Fig. 3.

The reasons for the quenching of the graphene Raman signal around the Si/SiGe HJ were investigated. For this, we solved the Maxwell equations for the NW/graphene/Al system; for more details, see Refs. 26–28. The Si/SiGe HJ is not abrupt, but it consists of a transition region where the composition varies gradually between Si and $Si_{1-x}Ge_x$ ($x \approx 0.6$), typically the HJ width lies between 10 and 30 nm depending on the growth conditions and the NW diameter.[33] Figure 4 shows the EM field distribution along a heterostructured NW with a 30 nm width HJ. The reference point on the Si segment is 200 nm away from the HJ. We can see in Fig. 4 that the EM mode distribution is radically different for the two situations. The Si segment shows a near two-lobe field distribution, while the field at the HJ is formed by just one localized lobe fully enclosed inside the NW. This electric field distribution inside the NW can account for the quenching of the Raman signal of graphene in the presence of the HJ. When the HJ is illuminated by the laser beam, the EM field on the HJ region is fully localized inside the NW, forming a single lobe pattern; in other words, the HJ is very efficient collecting the electromagnetic field. The optical mode is almost fully confined inside the NW; therefore, the electric field at the NW/graphene interface is very low, and the graphene layer is only weakly excited. Such electric field confinement does not take place for the homogeneous segments of the NW, where the electromagnetic field is enhanced at the NW/graphene interface with the

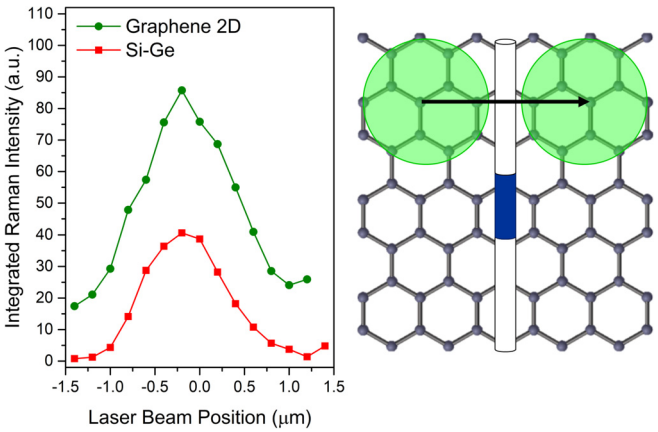

FIG. 2. Transversal Raman intensity profile of a SiGe/Si/SiGe NW over graphene lying on an Al substrate. The Si–Ge peak of SiGe is used as a reference of the NW signal and the 2D peak is the reference for graphene. The signals of the NW and graphene present a very good correlation evidencing the role of the NW in the enhancement of the Raman signal of graphene. A comparison of two Raman spectra inside and outside the NW enhancement effect is provided in Fig. S1.

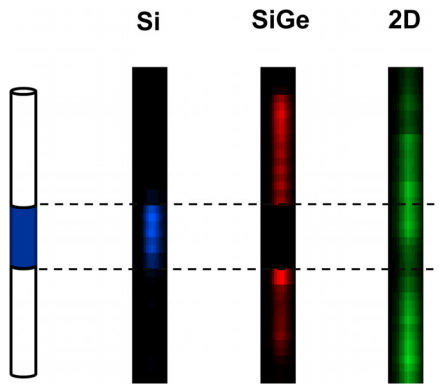

FIG. 3. 2D Raman mapping of a SiGe/Si/SiGe NW over graphene lying on an Al substrate, showing the Raman signals of Si (blue), SiGe (red), and graphene 2D (green) peaks. The enhancement on the lower HJ (leading) can be detected on the Si–Si (SiGe) signal (red). The graphene 2D band (green) is rather homogeneous throughout the NW presenting a minimum that coincides with the Si/SiGe HJ.

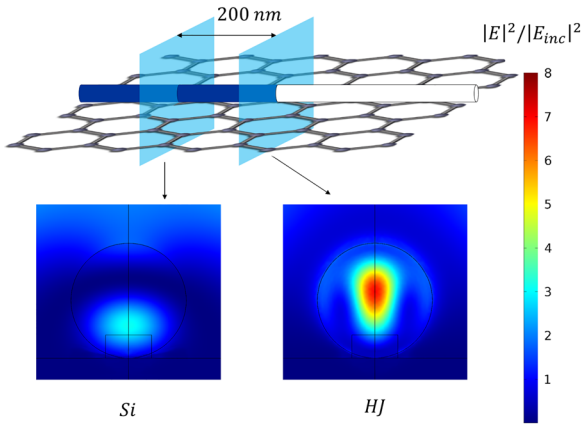

FIG. 4. EM field distribution for two different positions along the NW axis: Si segment and the HJ. The plane on the Si segment is 200 nm away from the HJ plane. The plot shows the localization of the EM on the NW center at the HJ, but not on the Si segment.

concomitant enhancement of the Raman signal of graphene. The localization of the EM field inside the NW at the HJ should account for the partial suppression of the Raman signal arising from graphene, as experimentally observed. Moreover, it evinces the light-harvesting capabilities of axially heterostructured NWs by confining the incident EM field in the NW interior, as well as the possibility to achieve a 3D localization of the EM field at a deep subwavelength scale inside the NW.

It is interesting to note that, of the two HJs, the SiGe/Si one (up) does not show local electric field enhancement, and therefore, the graphene signal at this HJ is not quenched (see Fig. 3). The different response of both HJs was previously observed, and it is the consequence of their different abruptness.[26,33] Furthermore, the absence of enhancement of the Raman signal of the SiGe/Si HJ is in good agreement with the absence of changes in the Raman signal of graphene when this HJ is illuminated.

In conclusion, semiconductor NWs are useful to enhance the optical response (monitored by the Raman signal) of a graphene layer deposited on a metal substrate. This recovery is related to the nanoantenna behavior of the NW, which localizes the electromagnetic field in the vicinity of the NW/graphene contact region, allowing for the retrieval of the Raman signal. Contrarily to the expected enhancement of the Raman signal of graphene, a quenching effect was observed when it is in contact with the Si/SiGe HJ. Even if it appears counterintuitive, due to the resonance absorption reported for the NW HJs, the results are in perfect agreement with the EM-FEM simulations. The model predicts a localization of the EM field inside the NW around the HJ region, almost vanishing at the NW/graphene contact region, which prevents the excitation of the Raman spectrum of graphene. The antenna behavior of the NW is able to localize the field in the NW radial direction, while the presence of axial HJs allows to control the excitation in the axial direction at a nanometric scale. As a result, it is possible to completely manage the 3D field localization of the EM field on a deep subwavelength scale by using different NW heterostructures, e.g., superlattices. This behavior can be tailored using different HJs, although further work is required to study the light trapping properties of different HJs. This light/matter interaction can be the basis for the application of semiconductor NWs as near-field probes for molecules or other materials near their surface.

See the supplementary material for a comparison of two Raman spectra inside and outside the NW enhancement effect.

AUTHORS' CONTRIBUTIONS

J.L.P. and J.J. wrote the manuscript and contributed equally to analyzing the results and in the writing process. O.B. performed the single-layer graphene growth and transfer. T.B. provided the heterostructured NWs.

This work was funded by Junta de Castilla y León (Project No. VA283P18) and the Spanish Government (No. ENE 2014-56069-C4-4-R). J. L. Pura was granted by the FPU program (Spanish Government) (No. FPU14/00916).

DATA AVAILABILITY

The data that support the findings of this study are available from the corresponding author upon reasonable request.

REFERENCES

[1]L. K. Van Vugt, B. Zhang, B. Piccione, A. A. Spector, and R. Agarwal, "Size-dependent waveguide dispersion in nanowire optical cavities: Slowed light and dispersionless guiding," Nano Lett. **9**(4), 1684–1688 (2009).
[2]D. Spirkoska, G. Abstreiter, and A. Fontcuberta I Morral, "Size and environment dependence of surface phonon modes of gallium arsenide nanowires as measured by Raman spectroscopy," Nanotechnology **19**(43), 435704 (2008).
[3]S. M. Bergin, Y. H. Chen, A. R. Rathmell, P. Charbonneau, Z. Y. Li, and B. J. Wiley, "The effect of nanowire length and diameter on the properties of transparent, conducting nanowire films," Nanoscale **4**(6), 1996–2004 (2012).
[4]X. Zhuang, C. Z. Ning, and A. Pan, "Composition and bandgap-graded semiconductor alloy nanowires," Adv. Mater. **24**(1), 13–33 (2012).
[5]M. Khorasaninejad, S. Patchett, J. Sun, N. O, and S. S. Saini, "Diameter dependence of polarization resolved reflectance from vertical silicon nanowire arrays: Evidence of tunable absorption," J. Appl. Phys. **114**(2), 024304 (2013).
[6]K. T. Fountaine, W. S. Whitney, and H. A. Atwater, "Resonant absorption in semiconductor nanowires and nanowire arrays: Relating leaky waveguide modes to Bloch photonic crystal modes," J. Appl. Phys. **116**(15), 153106 (2014).
[7]P. Yang, R. Yan, and M. Fardy, "Semiconductor nanowire: Whats next?," Nano Lett. **10**(5), 1529–1536 (2010).
[8]E. D. Minot, F. Kelkensberg, M. van Kouwen *et al.*, "Single quantum dot nanowire LEDs," Nano Lett. **7**(2), 367–371 (2007).
[9]F. Qian, Y. Li, S. Gradečak, D. Wang, C. J. Barrelet, and C. M. Lieber, "Gallium nitride-based nanowire radial heterostructures for nanophotonics," Nano Lett. **4**(10), 1975–1979 (2004).
[10]M. H. Huang, S. Mao, H. Feick, H. Yan, Y. Wu, H. Kind, E. Weber, R. Russo, and P. Yang, "Room-temperature ultraviolet nanowire nanolasers," Science **292**(5523), 1897–1899 (2001).
[11]X. Duan, Y. Huang, R. Agarwal, and C. M. Lieber, "Single-nanowire electrically driven lasers," Nature **421**(6920), 241–245 (2003).
[12]J. Wallentin, N. Anttu, D. Asoli *et al.*, "InP nanowire array solar cells achieving 13.8% efficiency by exceeding the ray optics limit," Science **339**(6123), 1057–1060 (2013).
[13]G. Otnes and M. T. Borgström, "Towards high efficiency nanowire solar cells," Nano Today **12**, 31–45 (2017).
[14]I. Aberg, G. Vescovi, D. Asoli *et al.*, "A GaAs nanowire array solar cell with 15.3% efficiency at 1 sun," IEEE J. Photovoltaics **6**(1), 185–190 (2016).
[15]J. E. M. Haverkort, E. C. Garnett, and E. P. A. M. Bakkers, "Fundamentals of the nanowire solar cell: Optimization of the open circuit voltage," Appl. Phys. Rev. **5**(3), 031106 (2018).

[16]T. Mårtensson, C. P. T. Svensson, B. A. Wacaser, M. W. Larsson, W. Seifert, K. Deppert, A. Gustafsson, L. R. Wallenberg, and L. Samuelson, "Epitaxial III−V nanowires on silicon," Nano Lett. **4**(10), 1987–1990 (2004).
[17]J. Anaya, S. Rossi, M. Alomari, E. Kohn, L. Tóth, B. Pécz, and M. Kuball, "Thermal conductivity of ultrathin nano-crystalline diamond films determined by Raman thermography assisted by silicon nanowires," Appl. Phys. Lett. **106**(22), 223101 (2015).
[18]C. N. Prinz, "Interactions between semiconductor nanowires and living cells," J. Phys. **27**(23), 233103 (2015).
[19]A. M. Munshi, D. L. Dheeraj, V. T. Fauske, D. C. Kim, A. T. J. Van Helvoort, B. O. Fimland, and H. Weman, "Vertically aligned GaAs nanowires on graphite and few-layer graphene: Generic model and epitaxial growth," Nano Lett. **12**(9), 4570–4576 (2012).
[20]Y. Ahn, Y. Jeong, D. Lee, and Y. Lee, "Copper nanowire-graphene core-shell nanostructure for highly stable transparent conducting electrodes," ACS Nano **9**(3), 3125–3133 (2015).
[21]D. Lee, H. Lee, Y. Ahn, Y. Jeong, D. Y. Lee, and Y. Lee, "Highly stable and flexible silver nanowire-graphene hybrid transparent conducting electrodes for emerging optoelectronic devices," Nanoscale **5**(17), 7750–7755 (2013).
[22]X. W. Fu, Z. M. Liao, Y. B. Zhou, H. C. Wu, Y. Q. Bie, J. Xu, and D. P. Yu, "Graphene/ZnO nanowire/graphene vertical structure based fast-response ultraviolet photodetector," Appl. Phys. Lett. **100**(22), 223114 (2012).
[23]D. Sinha and J. U. Lee, "Ideal graphene/silicon Schottky junction diodes," Nano Lett. **14**(8), 4660–4664 (2014).
[24]G. Fan, H. Zhu, K. Wang, J. Wei, X. Li, Q. Shu, N. Guo, and D. Wu, "Graphene/silicon nanowire Schottky junction for enhanced light harvesting," ACS Appl. Mater. Interfaces **3**(3), 721–725 (2011).
[25]C. Xie, J. Jie, B. Nie *et al.*, "Schottky solar cells based on graphene nanoribbon/multiple silicon nanowires junctions," Appl. Phys. Lett. **100**(19), 193103 (2012).
[26]J. L. Pura, J. Anaya, J. Souto, A. C. Prieto, A. Rodríguez, T. Rodríguez, P. Periwal, T. Baron, and J. Jiménez, "Electromagnetic field enhancement effects in group IV semiconductor nanowires. A Raman spectroscopy approach," J. Appl. Phys. **123**(11), 114302 (2018).
[27]J. L. Pura, J. Anaya, J. Souto, Á. C. Prieto, A. Rodríguez, T. Rodríguez, and J. Jiménez, "Local electric field enhancement at the heterojunction of Si/SiGe axially heterostructured nanowires under laser illumination," Nanotechnology **27**(45), 455709 (2016).
[28]J. L. Pura, J. Anaya, and J. Jiménez, "About the interaction between a laser beam and group IV nanowires: A study of the electromagnetic field enhancement in homogeneous and heterostructured nanowires," Phys. Status Solidi A **215**(19), 1800336 (2018).
[29]L. M. Malard, M. A. Pimenta, G. Dresselhaus, and M. S. Dresselhaus, "Raman spectroscopy in graphene," Phys. Rep. **473**(5-6), 51–87 (2009).
[30]A. C. Ferrari and D. M. Basko, "Raman spectroscopy as a versatile tool for studying the properties of graphene," Nat. Nanotechnol. **8**, 235–246 (2013).
[31]C. Casiraghi, S. Pisana, K. S. Novoselov, A. K. Geim, and A. C. Ferrari, "Raman fingerprint of charged impurities in graphene," Appl. Phys. Lett. **91**(23), 233108 (2007).
[32]J. L. Pura and J. Jiménez, "Fourier transform study of the complex electric field induced on axially heterostructured nanowires," Nanotechnology **30**(46), 465205 (2019).
[33]J. L. Pura, P. Periwal, T. Baron, and J. Jiménez, "Growth dynamics of SiGe nanowires by the vapour–liquid–solid method and its impact on SiGe/Si axial heterojunction abruptness," Nanotechnology **29**, 355602 (2018).